American Journal of Environmental Protection, 2022, Vol. 10, No. 2, 83-90
Available online at http://pubs.sciepub.com/env/10/2/5
Published by Science and Education Publishing
DOI:10.12691/env-10-2-5

Dynamic Adsorption and Desorption of CO_2 from Binary Mixtures of CH_4 and C_3H_8 on X Type Zeolites

Charly Mve Mfoumou[1,*], Pradel Tonda-Mikiela[1], Francis Ngoye[1], Thomas Belin[2], Samuel Mignard[2]

[1]Laboratoire de Chimie des Milieux et des Matériaux Inorganiques (LC2MI), URCHI / Université des Sciences et Techniques de Masuku (USTM), BP : 943 Franceville-Gabon
[2]Institut de Chimie des Milieux et Matériaux de Poitiers (IC2MP), UMR 7285 CNRS / Université de Poitiers, 4 Rue Michel Brunet, 86022 Poitiers Cedex, France
*Corresponding author: charly.mvemfoumou@univ-masuku.org

Received September 08, 2022; Revised October 12, 2022; Accepted October 24, 2022

Abstract Dynamic adsorption and desorption of carbon dioxide (CO_2) from binary gas mixtures (CO_2/CH_4 and CO_2/C_3H_8) was carried out on BaX and NaX zeolites in order to study the influence of methane and propane on the CO_2 adsorption capacities and on the preferential adsorption sites of CO_2. The adsorption proprieties of CH_4 and C_3H_8 molecules on the adsorbents were also evaluated. This study enabled to conclude that methane has no affinity with NaX and BaX zeolites in our experimental conditions. On the other hand, whatever the adsorbent studied, the results show favorable adsorption sites to trapping of propane. The adsorption capacities of propane at saturation on NaX and BaX zeolites are 0.035 and 0.075 mmol g^{-1} respectively. However, BaX zeolite is the adsorbent which presents more affinity for propane with the strongest propane/zeolite interactions. The study of CO_2 adsorption in presence CH_4 and C_3H_8 on the NaX zeolite indicates a decrease of the CO_2/cation interactions and of adsorbed CO_2 amounts at saturation. The capacities loss are about of 17% and 30% when carbon dioxide adsorption is carried out in binary mixture CO_2/CH_4 and CO_2/C_3H_8 respectively. In addition, a loss of preferential adsorption sites of carbon dioxide between 443 - 483 K is also observable in the presence of CH_4 on NaX zeolite. However on BaX zeolite, the presence of CH_4 and C_3H_8 improves the accumulation of CO_2 in the porosity. The capacities of CO_2 adsorption are improved about of 18% whatever the gas mixture studied. Moreover, contrary to NaX zeolite, a conservation of preferential adsorption sites of CO_2 on BaX zeolite in the temperature range studied (295 - 623 K) is visible. It seems that the presence of methane and propane doesn't affect the adsorption proprieties of carbon dioxide on BaX zeolite in our experimental conditions.

Keywords: *dynamic adsorption, Zeolite X, binary gas mixture, Carbon dioxide (CO_2) adsorption / desorption, Methane (CH_4), Propane (C_3H_8)*

Cite This Article: Charly Mve Mfoumou, Pradel Tonda-Mikiela, Francis Ngoye, Thomas Belin, and Samuel Mignard, "Dynamic Adsorption and Desorption of CO_2 from Binary Mixtures of CH_4 and C_3H_8 on X Type Zeolites." *American Journal of Environmental Protection*, vol. 10, no. 2 (2022): 83-90. doi: 10.12691/env-10-2-5.

1. Introduction

According to the latest report of the Intergovernmental Panel on Climate Change (IPCC), carbon dioxide (CO_2) and methane (CH_4) are the two main greenhouse gases (GHGs) responsible of the increase in global temperatures. Indeed, they represent more than 80% of GHG emissions, the majority of which come from fossil fuels [1]. In contrast, carbon dioxide concentrations are 220 times higher than methane concentrations in the atmosphere and have attained their highest level in recent years [1]. CO_2 is thus becoming the main cause of global warming. The urgency to find effective methods and techniques to limit CO_2 emissions into the atmosphere is necessary.

However, technologies are available to capture or separate CO_2 from industrial off-gases in order to limit its emissions [2,3]. Separation techniques such as chemical and physical absorption, cryogenics, membrane technology and physical adsorption are the most common in industry [2]. In contrast, adsorption techniques, using porous solids as adsorbent, appear to be the most effective for the capture and separation of CO_2 from flue gases [2,4,5,6]. Solids with three-dimensional porous structure, such as zeolites, are among the most suitable adsorbents for CO_2 capture or storage [7,8,9,10]. On the other hand, faujasite X type zeolites are the most used because of their large micropore volume [10-19].

Indeed, the improvement of such emission reduction and/or carbon dioxide recovery processes requires the search for adsorbents with high capacities of adsorption

and high selectivity of CO_2 in the presence of other gases (CH_4, H_2, N_2, H_2O,...) or impurities, low regeneration conditions and good stability in the adsorption/desorption processes. Known the characteristic CO_2 adsorption parameters of the adsorbents is also important in order to improve the selective trapping or separation of carbon dioxide in gas mixtures. Thus, several studies on the separation of carbon dioxide in gas mixtures using X-type zeolites have been conducted [20-27]. Studies on the selectivity of CO_2 in the presence of gases such as CH_4, H_2, O_2 and N_2 have been performed [20,21,25,26]. The influence of these gases on the diffusion and capacities of CO_2 adsorption was also evaluated. Other studies on the effect of the presence of water on the capacities of and preferential adsorption sites for CO_2 at low temperatures have also been carried out on faujasite X type zeolites [28,29]. However, all these studies do not show the influence of molecules such as CH_4 and C_3H_8 on the preferential CO_2 adsorption sites at low temperature and on the CO_2 adsorption capacities of X-type zeolites when the carbon dioxide is adsorbed in a binary gas mixture.

Therefore, the objective of this work is to study the influence of the presence of CH_4 and C_3H_8 on the adsorption capacities and on the preferential adsorption sites of CO_2 of NaX and BaX zeolites, during the adsorption of CO_2/CH_4 and CO_2/C_3H_8 gas mixtures. The diffusion of CO_2 into the porosity of the adsorbents as well as the affinity and maximum desorption temperatures of methane and propane molecules will also be evaluated. The fixed bed dynamic adsorption/desorption technique will be the main adsorption technique used in this study.

2. Experimental

2.1. Cationic Exchange

The starting material is a NaX zeolite supplied by Axens. The replacement of the sodium cations by barium cations has been obtained by cationic exchange, using barium nitrate $Ba(NO_3)_2$ from Sigma-Aldrich (purity > 99%). Cationic exchange was carried out at 343 K by stirring 3 g of zeolites powder in 250 mL of aqueous solution containing $[Ba^{2+}]$ = 0.02 mol.L^{-1} of the metal nitrate for 24 h. The sample was then filtered, washed with ultrapure water (3 x 40 mL) to eliminate the free nitrate ions into the solids. It was then dried in a furnace during 24 h at 373 K. Exchanged BaX zeolite was finally sieved to obtain a particle size between 0.2 and 0.4 mm.

2.2. Characterizations

Elemental analysis of M-X zeolites was performed by ICP to quantify the amounts of ion-exchanged cation species.

The thermal stability (mass loss) was performed on an SDT-Q-600 TA instrument with a stream of dry argon (100 mL.min^{-1}) in a temperature range between 298 and 1073 K, using a ramp of 5 K.min^{-1}.

Measurements of surface area and pore volume were carried out using a Micromeritics TRISTAR 3000 instrument. About 100-150 mg of the zeolite sample was pretreated during 1 h at 363 K, then 10 h at 623 K. The adsorption/desorption isotherm of nitrogen was carried out at 77 K. The specific surface areas of samples were evaluated by means of the Brunauer, Emmett and Teller (BET) theory [30]. Microporous and mesoporous volumes were determined by *t*-plot method of De Boer and Dubinin-Radushkevich equation respectively [31,32,33].

X-Ray Diffraction (XRD) patterns were recorded at room temperature on a Siemens D5005 diffractometer using Cu Kα monochromatic radiation with 0.154050 nm wavelength. The samples were scanned in the 3 - 70° (2θ) range with a 0.01°/s step.

2.3. Gases Binary Mixture Adsorption and Desorption

For the adsorption experiments in fixed-bed dynamic, the total gas flow at the entry and in exit of the reactor is fixed at 150 mL.min^{-1}. The concentration of each gas (CO_2, CH_4 and C_3H_8) is of 900 ppm and the gases flow is of 14 mL.min^{-1} for each gas in order to obtain a concentration applied in entry of the reactor of 84 ppm. To obtain the fixed total flow (150 mL.min^{-1}), any difference is completed by a reconstituted air flow. Adsorption experiments were carried out at room temperature (295 K) with a bed height of 2.9 cm (550-650 mg of adsorbents).

Desorption experiments were carried out on the same bed of adsorbent, once this one was saturated. The principle is based on the sending of air reconstituted in entry of the reactor (flow: 80 mL.min^{-1}) with a simultaneous heating of the sample following a ramp of 24 K.min^{-1} until 623 K. The desorbed compounds are analyzed on line using the chromatograph in gas phase and the gaseous composition in exit of the reactor.

3. Theoretical Aspects

The composition of the gas mixture outflow of the adsorbents bed is analyzed every four minutes. It is thus possible to plot the curve of drilling corresponding to each gas. These curves translate the efficiency of the bed to trap or adsorb a gas. The saturation of bed is reached when the concentrations at exit of the reactor (C) are equal to the values of the concentrations of the "blank" (C_0) that is the ratio C/C_0 equal to the unit. We obtain surface areas in minute, from integration by trapeze method:

$$A = \sum_i \frac{\left(t_{i+1} - t_i\right) \cdot \left(2 - \frac{C_{i+1}}{C_0} - \frac{C_i}{C_0}\right)}{2}$$

C_0 and C_i are the concentrations of gas at the entry and outflow of the reactor at time T_i, respectively. In addition, the quantity of gas adsorbed (q) in the bed is given by relation:

$$q\left(mol/g\right) = \frac{D \times A_i \cdot \left(\frac{10^{-7} \times C_i \times P}{R \times T}\right)}{m_i}$$

where D, C_i, P, R, T and A_i correspond to the total flow of the gas mixture (mL min^{-1}), the concentration of the adsorbate (I) in entry of the reactor (ppm), the atmospheric

pressure (bar), the perfect gas constant (J K mol^{-1}), the temperature (K) and the surface areas corresponding to the adsorbed quantity (min), respectively.

4. Results and Discussion

The discussions on the results of characterizations of studied adsorbents (BaX and NaX) were detailed in a recent article on the study of preferential adsorption sites of H_2O on adsorption sites of CO_2 at low temperature onto NaX and BaX zeolites [28].

4.1. CO_2 Adsorption in Gas Mixture in Fixed-bed Dynamic

CO_2 adsorption from gas mixtures (CO_2/CH_4 and CO_2/C_3H_8) on NaX and BaX zeolites was carried out in fixed-bed dynamic to study the influence of molecules of neighboring size and molecular weight of carbon dioxide (CH_4 and C_3H_8, respectively) on the CO_2 adsorption capacities and the diffusion of the CO_2 molecule into the pores of the adsorbents. The adsorption capacities of methane and propane were also determined to evaluate the pore diffusion and affinity of gases with the studied adsorbents.

4.1.1. Adsorption of Binary Mixture CO_2/CH_4

Table 1 shows the amounts of the adsorbed gases (CO_2 and CH_4) of gas mixture CO_2/CH_4 obtained on NaX and BaX zeolites. Those obtained during the adsorption of carbon dioxide only ($CO_{2\ ref.}$), obtained in a recent study are also listed as reference [28]. The amounts of CO_2 adsorbed before breakthrough and at saturation on NaX zeolite (0.128 and 0.144 mmol.g^{-1} respectively) are lower than the amounts determined in the case of the adsorption of CO_2 only (Table 1).

Table 1. Adsorption capacities in gas mixture (CO_2/CH_4) obtained at 295 K in fixed-bed-dynamic on NaX and BaX zeolites. CO_2 amounts obtained during the adsorption of CO_2 only are also reported as reference [28]

Adsorbents	Amounts adsorbed (mmol.g^{-1})					
	Before breakthrough			At saturation		
	$CO_{2\ ref.}$	CO_2	CH_4	$CO_{2\ ref.}$	CO_2	CH_4
NaX	0.161	0.128	0	0.173	0.144	0.004
BaX	0.067	0.078	0	0.093	0.110	0.003

The NaX zeolite loses about 17% of the CO_2 adsorption capacities in the presence of CH_4. Methane seems to limit the accumulation of carbon dioxide in the pores of the NaX zeolite and / or limit the CO_2/cation interactions since the CO_2 adsorption takes place principally on cationic sites.

Unlike NaX, BaX zeolite increases the CO_2 adsorption capacities of 18% in presence of CH_4. Indeed, the amounts of CO_2 adsorbed obtained in adsorption of binary mixture before breakthrough and at saturation (0.078 and 0.110 mmol.g^{-1} respectively) are higher than those obtained in CO_2 adsorption only (0.067 and 0.093 mmol.g^{-1} respectively) as shown in Table 1. The presence of CH_4 seems to improve the accumulation of the CO_2 molecule in the pores of BaX zeolite.

The capacities of methane adsorption are practically similar for both adsorbents (Table 1). However, compared to the adsorption capacities of CO_2, CH_4 is not adsorbed on adsorbents studied. In fact, the quantities of CH_4 adsorbed are very small or negligible. These values are in the range of the experimental error (3.10^{-3} mmol.g^{-1}).Thus, BaX and NaX zeolites show no affinity with methane in our experimental conditions. The recent research of Supatsorn Parinyakit *et al*. also indicated a low affinity of methane with 13X zeolite during the adsorption of the binary gas mixture CO_2/CH_4 [34].

The Figure 1 shows the breakthrough curves in the CO_2/CH_4 binary mixture obtained on NaX zeolite. The breakthrough curve obtained in CO_2 adsorption only is also reported as reference. As expected, CH_4 has no affinity with NaX zeolite. The breakthrough is immediate on this zeolite.

The CO_2 breakthrough time obtained on NaX zeolite for the breakthrough curves of CO_2 adsorption in binary mixture is nearly similar compared to that obtained with CO_2 adsorption only (Figure 1). However, the slopes of breakthrough curves obtained when the bed is saturated are slightly different. This slight variation could indicate a slower diffusion of carbon dioxide molecule in the pores of NaX zeolite in the presence of methane or the weak interactions between CO_2 and cationic sites. The decrease in the slope of the CO_2 adsorption breakthrough curve in binary mixture confirms these observations. Indeed, the presence of methane decreases the capacities of CO_2 adsorption and modifies the diffusion of carbon dioxide in the porosity of the NaX zeolite.

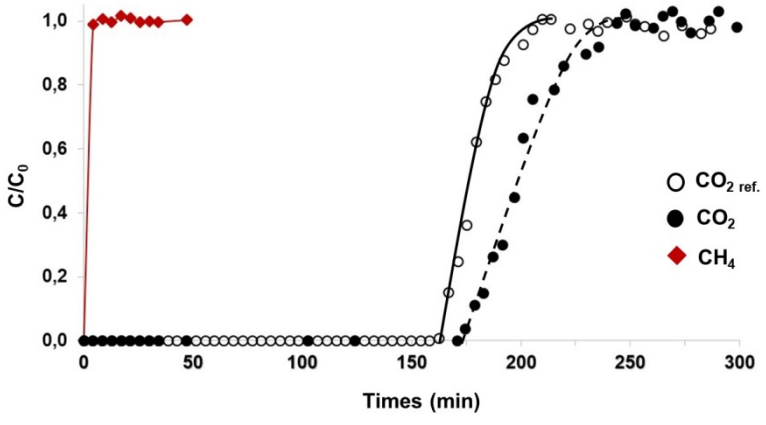

Figure 1. Breakthrough curves of carbon dioxide (85 ppm) and methane (85 ppm) obtained on NaX in fixed-bed dynamic at 295 K for the adsorption of the binary mixture CO_2/CH_4. The curve corresponding to the adsorption of CO_2 only ($CO_{2\ ref.}$) is presented for comparison

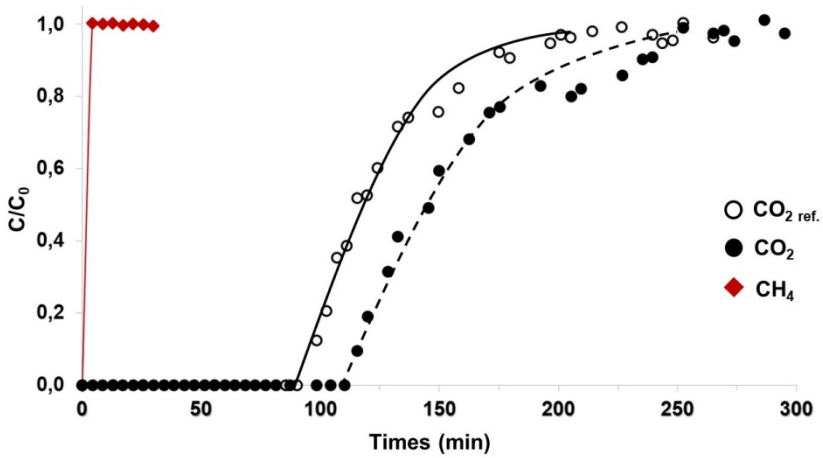

Figure 2. Breakthrough curves of carbon dioxide (85 ppm) and methane (85 ppm) obtained on BaX in fixed-bed dynamic at 295 K for the adsorption of the binary mixture CO_2/CH_4. The curve corresponding to the adsorption of CO_2 only ($CO_{2\ ref.}$) is presented for comparison

The CO_2/CH_4 binary mixture breakthrough curves obtained on BaX are shown in Figure 2. The breakthrough curve obtained in CO_2 adsorption only is also reported as reference. As shown by the capacity at saturation, the breakthrough of methane is very fast as in the experiment with NaX zeolite.

The breakthrough time of CO_2 from binary mixture is higher than that obtained for CO_2 alone (Figure 2). As opposed to NaX zeolite, the slopes of the breakthrough curves are similar in both cases. The diffusion of CO_2 into the pores of BaX zeolite does not seems to be modified in the presence of CH_4. Thus, the presence of methane increases the adsorption capacities on BaX zeolite (Table 1) and has no effect on the diffusion of carbon dioxide into the pores of this adsorbent.

4.1.2. Adsorption of Binary Mixture CO_2/C_3H_8

Table 2 lists the capacities of adsorption of CO_2 and C_3H_8 obtained on the NaX and BaX zeolites. Contrary to methane, propane is adsorbed by the adsorbents studied. There are thus adsorbate-adsorbent interactions between these materials and propane.

Table 2. Adsorption capacities in gas mixture (CO_2/C_3H_8) obtained at 295 K in fixed-bed dynamic on NaX and BaX zeolites. CO_2 amounts obtained during the adsorption of CO_2 only are also reported as reference [28]

Adsorbents	Capacities adsorbed (mmol.g^{-1})					
	Before breakthrough			At saturation		
	$CO_{2\ ref}$	CO_2	C_3H_8	$CO_{2\ ref}$	CO_2	C_3H_8
NaX	0.161	0.104	0.007	0.173	0.115	0.035
BaX	0.067	0.079	0.035	0.093	0.094	0.072

The adsorbed C_3H_8 amounts before breakthrough and at saturation obtained on NaX zeolite are 0.007 and 0.035 mmol.g^{-1} respectively. These amounts of C_3H_8 adsorbed on NaX are lower compared to those obtained on BaX zeolite before breakthrough (0.035 mmol.g^{-1}) and at saturation (0.072 mmol.g^{-1}). It seems as on BaX zeolite, the propane/adsorbent interactions are more important.

As in presence of CH_4, the adsorbed CO_2 amounts before breakthrough and at saturation obtained on NaX (0.104 and 0.115 mmol.g^{-1} respectively) are lower than those obtained when trapping CO_2 alone. The percentage loss of CO_2 adsorption capacity in presence of C_3H_8 is estimated to be around 30%. It thus appears that on NaX zeolite, the presence of a molecule with a molar mass close to CO_2 affects more strongly the capacities of CO_2 adsorption.

However on BaX zeolite, the adsorbed CO_2 amounts before breakthrough (0.079 mmol.g^{-1} and at saturation (0.094 mmol.g^{-1}) are similar to those obtained with methane (Table 1). As in the case of methane, the presence of propane improves the accumulation of CO_2 in the porosity of BaX zeolite in our experimental conditions. In addition, the adsorbed CO_2 amounts are near to those obtained on the NaX zeolite at saturation (Table 2).

The breakthrough curves of CO_2 and C_3H_8 obtained on NaX zeolite are shown in Figure 3. For comparison, curve obtained when trapping CO_2 alone ($CO_{2\ ref}$) is also shown. The breakthrough curve of C_3H_8 shows a steep slope, indicating weak interactions between C_3H_8 and NaX zeolite and / or rapid diffusion of the methane molecule into the porosity of the NaX faujasite.

Furthermore, no desorption of C_3H_8 due to CO_2 is observed. This means that there is no competitive adsorption between propane and carbon dioxide. However, NaX zeolite remains more efficient for the capture of carbon dioxide in a binary mixture CO_2/C_3H_8 in our experimental conditions (Table 2).

Nevertheless, a decrease in the breakthrough time for CO_2 in the presence of C_3H_8 is visible by comparing with the breakthrough curve of CO_2 adsorption alone (Figure 3). Moreover, the slopes of the CO_2 breakthrough curves obtained in binary mixture or alone are similar. This indicates that the presence of propane does not affect the diffusion of CO_2 in the porosity of the NaX zeolite. Thus, the presence of propane during CO_2 trapping decreases only the efficiency of the NaX zeolite.

The BaX zeolite, on the other hand, shows a strong adsorption of C_3H_8 with strong interactions between propane and the zeolite structure as shown in Figure 4. Indeed, the breakthrough time of C_3H_8 (50 min) is higher than that obtained on the NaX faujasite (8 min). The adsorption capacities calculated confirm these results (Table 2). These observations suggest that there are more favorable sites for C_3H_8 adsorption on BaX adsorbent.

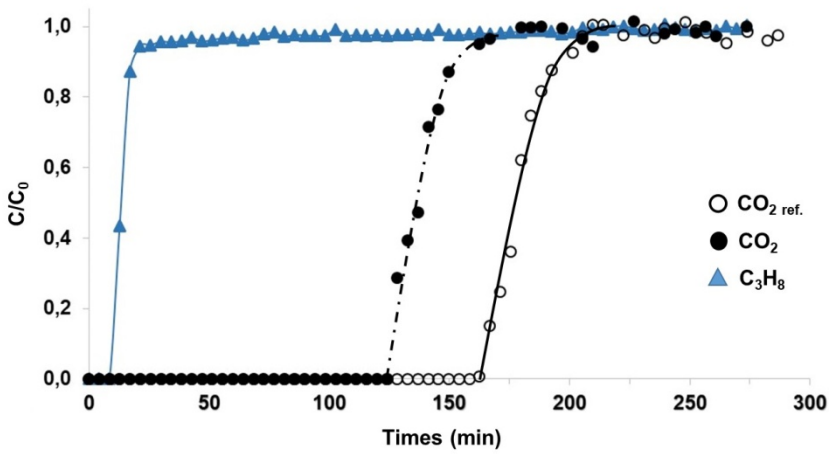

Figure 3. Breakthrough curves of carbon dioxide (85 ppm) and propane (85 ppm) obtained on NaX in fixed-bed dynamic at 295 K for the adsorption of the binary mixture CO_2/C_3H_8. The curve corresponding to the adsorption of CO_2 only ($CO_{2\ ref.}$) is presented for comparison

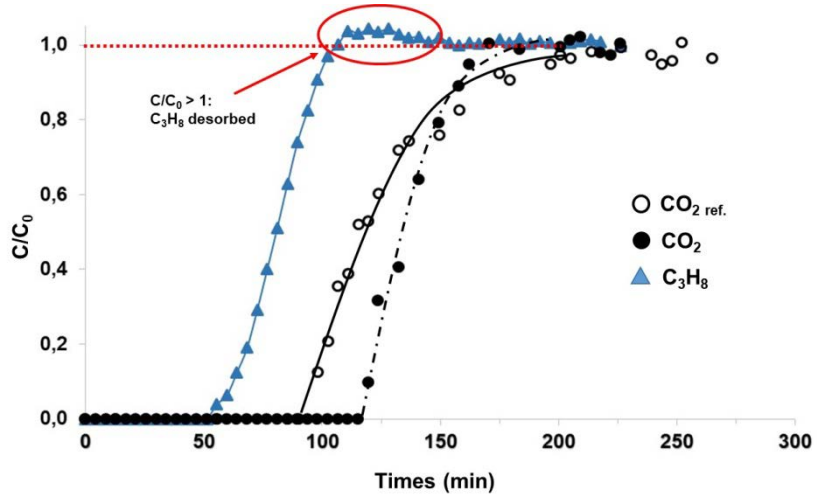

Figure 4. Breakthrough curves of carbon dioxide (85 ppm) and propane (85 ppm) obtained on BaX in fixed-bed dynamic at 295 K for the adsorption of the binary mixture CO_2/C_3H_8. The curve corresponding to the adsorption of CO_2 only ($CO_{2\ ref.}$) is presented for comparison

However, as opposed to NaX zeolite, a slight desorption of propane is visible ($C/C_0 > 1$). There is thus a competitive adsorption between carbon dioxide and propane on the BaX zeolite (Figure 4). It seems that on BaX zeolite, CO_2 has preferential adsorption sites that C_3H_8 cannot occupy. Nevertheless, the presence of propane does not disturb the capacities of saturation adsorption of carbon dioxide in the BaX adsorbent. Also contrary to CH_4 molecule, in the presence of C_3H_8 molecule, the slope of CO_2 breakthrough curve for adsorption of CO_2/C_3H_8 mixture (Figure 4) is different from that obtained when trapping CO_2 alone ($CO_{2\ ref}$). This reflects a more rapid diffusion of CO_2 in the porosity.

Thus, BaX zeolite can be used in selective adsorption or gas separation processes of C_3H_8 from gas effluents containing C_3H_8 with low gas concentrations. Indeed, this adsorbent presents favorable adsorption sites for propane. This result needs to be confirmed in the desorption study of CO_2 and C_3H_8.

4.2. Desorption of Gases Adsorbed

Desorption of the gases, once the beds were saturated, was carried out to study the effect of CH_4 and C_3H_8 molecules on the preferential adsorption sites of carbon dioxide, mainly at low temperature (295 – 623 K) on NaX and BaX zeolites. The affinity of the gases with the adsorbents was also evaluated.

4.2.1. Influence of CH_4

Figure 5 shows the evolution of the percentage of desorbed CO_2 and CH_4 obtained when the temperature increases obtained on NaX zeolite during the adsorption of the binary mixture CO_2/CH_4. For comparison, that obtained when trapping CO_2 alone ($CO_{2\ ref}$) is also shown.

No CH_4 is observed in the desorption profiles obtained. Methane is therefore not adsorbed in the NaX zeolite, as shown by the adsorption capacities calculated (Table 1).

The CO_2 desorption curve in binary mixture shows the same distribution of adsorption sites as that obtained when the CO_2 was desorbed alone (Figure 5). On the other hand, a temperature shift of the desorption profile in the range 295 – 483 K is observed. This corresponds to a loss of the preferential CO_2 adsorption sites between 463 - 483 K. This result could be explained by the fact that methane limits the accessibility of CO_2 to these sites. On the other hand, at high temperatures (573 – 623 K), the quantities desorbed remain similar (Figure 5). According to the results, in NaX zeolite, the presence of CH_4 molecule does not modify the proportions of desorbed CO_2. However, the temperature distribution of the physisorbed carbon dioxide species is decreased.

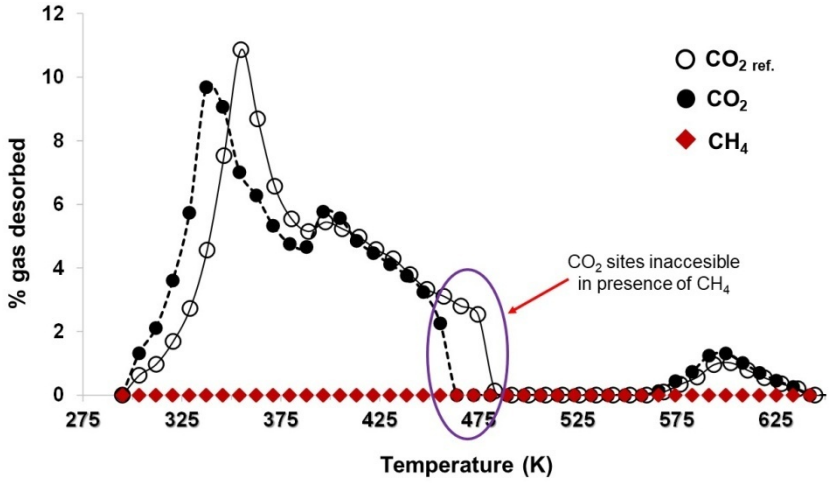

Figure 5. Desorption curves of CO_2 and CH_4 obtained at 24 k min^{-1} in fixed-bed dynamic on NaX zeolite. The curve corresponding to the desorption of CO_2 alone ($CO_{2\,ref.}$) is presented for comparison

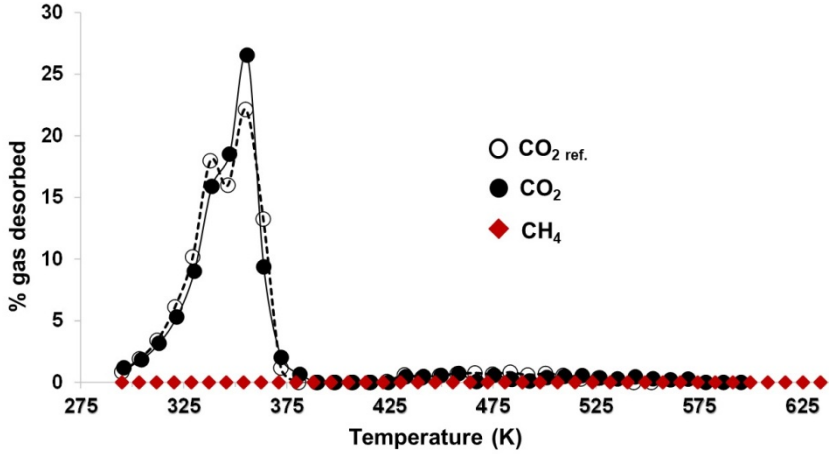

Figure 6. Desorption curves of CO_2 and CH_4 obtained at 24 k min^{-1} in fixed-bed dynamic on BaX zeolite. The curve corresponding to the desorption of CO_2 alone ($CO_{2\,ref.}$) is presented for comparison

On the BaX zeolite, the desorption curves obtained are showed in Figure 6. As with NaX, methane is not detected during the desorption. The quantities adsorbed are indeed very small (Table 1).

The desorption curves of CO_2 in mixture or alone ($CO_{2\ ref}$) are similar (Figure 6). No modification of desorbed species proportions and temperature shift in the distribution of CO2 preferential adsorption sites is observed in the range of temperatures explored. This confirms the capacity of the breakthrough curves. Methane does not disturb the distribution of CO_2 adsorption sites and does not interfere with the access of carbon dioxide to its preferential adsorption sites on the BaX zeolite.

4.2.2. Influence of C_3H_8

Desorption curves of carbon dioxide and propane obtained on NaX and BaX are shown in Figure 7 and Figure 8. The CO_2 desorption profile obtained when trapping CO_2 alone ($CO_{2\,ref}$) is also shown.

The curve obtained on the NaX zeolite shows a desorption of C_3H_8 in the temperature range between 295 – 333 K with a maximum of desorption around 323 K (Figure 7). There are thus, on the zeolite NaX, sites favorable to the adsorption of propane.

The desorption curve for CO_2 in the CO_2/C_3H_8 binary mixture (Figure 7) shows a distribution of desorbed CO_2 percentages similar to that obtained for CO_2 alone. As with the CH_4 profile (Figure 5), an offset (283 K) of temperature of the desorption maximum is observable. This temperature corresponds to the end of desorption of C_3H_8. It appears thus that CO_2 occupies different adsorption sites than propane. A decrease in the proportions of desorbed species (CO_2) between 343 - 483 K is also observed. Therefore, the loss of CO_2 capacity obtained in the presence of C_3H_8 could be attributed to the decrease of trapped species in this temperature range. Propane has thus made some sites inaccessible to CO_2.

For BaX zeolite (Figure 8), the curves of CO_2 and C_3H_8 show a desorption in the same temperature range (295 – 373 K). This result confirms that methane interacts more strongly with the BaX zeolite than with NaX. Indeed, the temperature at the desorption maximum is 356 K with a total desorption around 373 K. As in the case of methane, the distribution of preferential adsorption sites of CO_2 in the presence of methane does not appear to be modified on BaX (Figure 8). However, between 423 – 532 K, a weak desorption of CO_2 is still observable. These species are probably adsorbed on strong sites. The presence of C_3H_8 does not therefore disturb the access of carbon dioxide to these preferential adsorption sites.

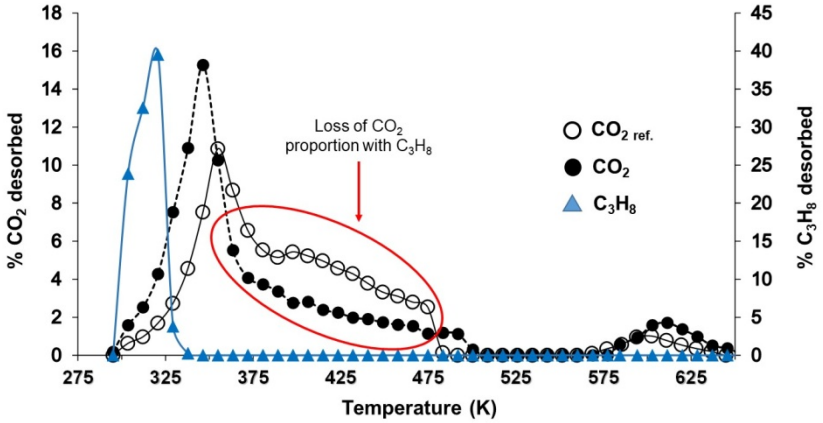

Figure 7. Desorption curves of CO_2 and C_3H_8 obtained at 24 k min^{-1} in fixed-bed dynamic on NaX zeolite. The curve corresponding to the desorption of CO_2 alone ($CO_{2\,ref.}$) is presented for comparison

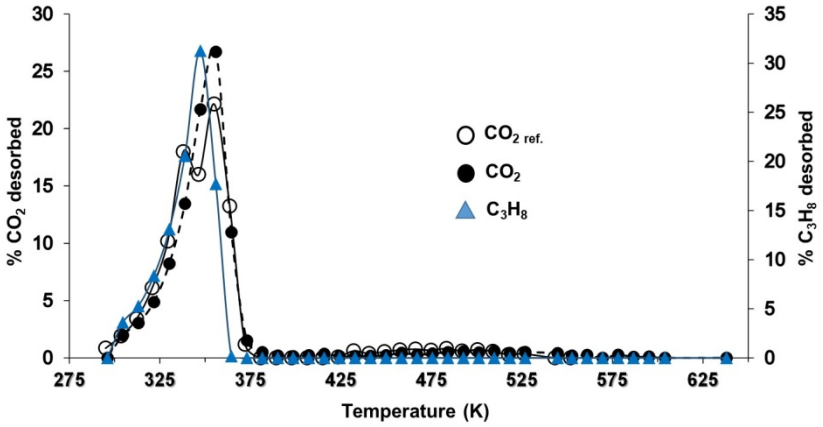

Figure 8. Desorption curves of CO_2 and C_3H_8 obtained at 24 k min^{-1} in fixed-bed dynamic on BaX zeolite. The curve corresponding to the desorption of CO_2 alone ($CO_{2\,ref.}$) is presented for comparison

5. Conclusion

The dynamic adsorption and desorption of carbon dioxide (CO_2) in gas mixtures with methane (CH_4) and propane (C_3H_8) at low gas concentration (84 ppm) was carried out on BaX and NaX zeolites in order to study the influence of molecules with sizes and molecular weights similar to those of carbon dioxide (CH_4 and C_3H_8 respectively) on: the capacities of carbon dioxide adsorption, the diffusion of CO_2 into the porosity of the adsorbents and/or the CO_2-adsorbent interactions and on the adsorption sites preferential of CO_2 in the temperature range of physisorbed carbon dioxide (295 - 623 K). The affinity and adsorption capacities of CH_4 and C_3H_8 on the adsorbents was also evaluated.

The capacities of CH_4 at saturation obtained on NaX and BaX zeolites (0.004 and 0.003 $mmol.g^{-1}$ respectively) are insignificant. It seems that CH_4 molecule has no affinity with NaX and BaX zeolites in our experimental conditions. The breakthrough and desorption curves of CH_4 obtained confirm the conclusions. On the other hand, whatever the adsorbent studied, the results obtained show favorable adsorption sites to the trapping of C_3H_8 molecule. The adsorption capacities of propane at saturation on NaX and BaX zeolites are 0.035 and 0.075 $mmol.g^{-1}$ respectively. It appears that BaX zeolite is the adsorbent which presents more affinity for C_3H_8 molecule and the strongest propane/zeolite interactions. Indeed, the exploitation of the desorption curves of C_3H_8 reveals on BaX, the temperatures of the maximum desorption peak (356 K) and total desorption of propane (373 K) higher than those obtained on NaX zeolite (320 and 338 K respectively).

The results of CO_2 adsorption in the presence of methane and propane on NaX zeolite indicate a decrease in the CO_2 / cation interactions, marked by a loss of capacities of about 17% and 30% when carbon dioxide trapping is carried out in binary mixture CO_2/CH_4 and CO_2/C_3H_8 respectively. Moreover, in the presence of methane, the CO_2 desorption study shows a loss of preferential adsorption sites of CO_2 between 443 - 483 K.

However on BaX zeolite, the presence of CH_4 and C_3H_8 improves the accumulation of CO_2 in the porosity. Indeed, the capacities of CO_2 adsorption are improved of about 18% whatever the binary mixture of gas studied. Though, the diffusion of CO_2 in the porosity of BaX zeolite is modified only in the presence of C_3H_8.

Moreover, as opposed to NaX zeolite, the CO_2 desorption study indicates a conservation of preferential adsorption sites of CO_2 on BaX zeolite in the temperature range between 295 - 623 K, whatever the gas effluent studied.

Therefore, in the presence of methane and propane, BaX zeolite keeps all its properties in the selective adsorption of carbon dioxide in this study. Thus, BaX zeolite can be used in the selective adsorption (gas separation) or valorization processes of C_3H_8 from effluents with low gas concentrations. Indeed, it presents

favorable adsorption sites for propane with low total desorption temperatures that are advantageous for adsorbent regeneration treatments.

Acknowledgments

This study was financially supported by the Research Program of the Université des Sciences et Techniques de Masuku and the Université de Poitiers.

Declaration of Conflicting Interests

The author(s) declared no potential conflicts of interest with respect to the research, authorship, and/or publication of this article.

References

[1] Groupe d'experts intergouvernemental sur l'évolution du climat (GIEC), *Synthèse du rapport AR6 du GIEC*, publié le 09/08/2021.

[2] A.A. Olajire, *CO2 capture and separation technologies for end-of-pipe applications* – A review, Energy, 35 (2010) 2610-2628.

[3] S. Akerboom, S. Waldmann, A. Mukherjee, C. Agaton, M. Sanders and G. Jan Kramer, *Different This Time? The Prospects of CCS in the Netherlands in the 2020s*, Frontiers in Energy Research, May 2021 | Volume 9 | Article 644796.

[4] A. Awadallah-F, F. Hillman, S. A. Al-Muhtaseb, H. K. Jeong, *Adsorption of Carbon Dioxide, Methane, and Nitrogen Gases onto ZIF Compounds with Zinc, Cobalt, and Zinc/Cobalt Metal Centers*, Journal of Nanomaterials, vol. 2019, Article ID 6130152, 11 pages, 2019.

[5] P-H. Huang, J-W Jhan, Y-M. Cheng, H-H. Cheng, *Effects of Carbonization Parameters of Moso-Bamboo-Based Porous Charcoal on Capturing Carbon Dioxide*, The Scientific World Journal, vol. 2014, Article ID 937867, 8 pages, 2014.

[6] P. Saisuwansiri, P. Worathanakul, *A Study of CO2 Thermodynamic Adsorption and Desorption with Bi-Metal Loading on Zeolite Y*, Materials Today: Proceedings, Volume 17, Part 4, 2019, Pages 1458-1465,

[7] I. Domínguez, J. Pawlesa, A. Zukal, J. Čejka, *Ferrierite and MCM-22 for the CO2 adsorption*, Surface Science and Catalysis, Volume 174, Part A, 2008, Pages 603-606.

[8] R. Girimonte, B. Formisani, F. Testa, *Adsorption of CO2 on a confined fluidized bed of pelletized 13X zeolite*, Powder Technology, Volume 311, 2017, Pages 9-17.

[9] C. Coelho, A. S. Oliveira, M. F. R. Pereira, O. C. Nunes, *J. Hazard. Mater.* B 138 (2006) 343.

[10] T. Belin, C. Mve Mfoumou, S. Mignard, Y. Pouilloux, *Study of physisorbed carbon dioxide on zeolites modified by addition of oxides or acetate impregnation*, Microporous and Mesoporous Materials, 182 (2013) 109-116.

[11] H. Hammoudi, S. Bendenia, K. Marouf-Khelifa, R. Marouf, J. Schott, A. Khelifa, *Micropor. Mesopor. Mat.* 113 (2008) 343.

[12] L. Jian-Rong, M. Yuguang, M. C. McCarthy, J. Sculley, J. Yu, H. K. Jeong, P. B. Balbuena, Z. Hong-Cai, *Coordin. Chem. Rev.* 255 (2011) 1791.

[13] H. Hammoudi, S. Bendenia, K. Marouf-Khelifa, R. Marouf, J. Schott, A. Khelifa, *Micropor. Mesopor. Mat.* 113 (2008) 343.

[14] A. Zukal, C. O. Arean, M. R. Delgado, P. Nachtigall, A. Pulido, J. Mayerova, J. Cejka, *Micropor. Mesopor. Mat.* 146 (2011) 97.

[15] S. Choi, J. H. Drese, C. W. Jones, *ChemSusChem* 2 (2009) 796.

[16] D. Bonnefant, M. Kharoune, P. Niquette, M. Mimeault, R. Hausler, *Sci. Techno. Adv. Mater*. 9 (2008) 13007.

[17] G. Calleja, J. Pau, J. A. Calles, *J. Chem. Eng.* 43 (1998) 994.

[18] J. Dunne, A. L. Myers, *Chem. Eng. Sci.* 49 (1994) 2941.

[19] J. A. Dunne, M. Rao, S. Sircar, R. J. Gorte, A. L. Myers, *Langmuir* 12 (1996) 5896.

[20] Shang, Jin and Hanif, Aamir and Li, Gang and Xiao, Gongkui and Liu, Jefferson Zhe and Xiao, Penny and Webley, Paul A., *Separation of CO2 and CH4 by Pressure Swing Adsorption Using a Molecular Trapdoor Chabazite Adsorbent for Natural Gas Purification*, Ind. Eng. Chem. Res, 2020, 59, 16, 7857-7865.

[21] Delgado, José A. and Águeda, V. I. and Uguina, M. A. and Sotelo, J. L. and Brea, P. and Grande, Carlos A., *Adsorption and Diffusion of H2, CO, CH4, and CO2 in BPL Activated Carbon and 13X Zeolite: Evaluation of Performance in Pressure Swing Adsorption Hydrogen Purification by Simulation*, Ind. Eng. Chem. Res. 2014, 53, 40, 15414-15426.

[22] Cavenati, Simone and Grande, Carlos A. and Rodrigues, Alírio E., *Adsorption Equilibrium of Methane, Carbon Dioxide, and Nitrogen on Zeolite 13X at High Pressures*, J. Chem. Eng. Data 2004, 49, 4, 1095-1101.

[23] Chue, K. T. and Kim, J. N. and Yoo, Y. J. and Cho, S. H. and Yang, R. T., *Comparison of Activated Carbon and Zeolite 13X for CO2 Recovery from Flue Gas by Pressure Swing Adsorption*, Ind. Eng. Chem. Res. 1995, 34, 2, 591-598.

[24] J-J. Kim, S-H. Hong, D. Park, K. Chung, C-H. Lee, *Separation of propane and propylene by desorbent swing adsorption using zeolite 13X and carbon dioxide*, *Chemical Engineering Journal*, Vol. 410, 2021, 128276.

[25] H. Moradi, H. Azizpour, H. Bahmanyar, M. Emamian, *Molecular dynamic simulation of carbon dioxide, methane, and nitrogen adsorption on Faujasite zeolite*, Chinese Journal of Chemical Engineering, Volume 43, 2022, Pages 70-76.

[26] M. Jaschik, M. Tanczyk, J. Jaschik, A. Janusz-Cygan, *Data concerning adsorption equilibria of carbon dioxide, nitrogen and oxygen over a zeolite molecular sieve 13X for the modelling of carbon dioxide capture from gaseous mixtures by adsorptive processes*, Data in Brief, Volume 30, 2020, 105638.

[27] M. C. Campo, A. M. Ribeiro, A. F.P. Ferreira, J. C. Santos, C. Lutz, J. M. Loureiro, A. E. Rodrigues, *Carbon dioxide removal for methane upgrade by a VSA process using an improved 13X zeolite*, Fuel Processing Technology, Volume 143, 2016, Pages 185-194.

[28] C.Mve Mfoumou, S. Mignard, T. Belin, *The preferential adsorption sites of H2O on adsorption sites of CO2 at low temperature onto NaX and BaX zeolites*, Adsorption Science & Technology, 36 (2018) 1246-1259.

[29] V. R. Mollo-Varillas, F. Bougie, M. C. Iliuta, *Selective adsorption of water vapor in the presence of carbon dioxide on hydrophilic zeolites at high temperatures*, Separation and Purification Technology, Volume 282, Part B, 2022, 120008.

[30] S. Brunauer, P.H. Emmett, E.J. Teller, J. Am. Chem. Soc. 60 (1938) 309.

[31] B.C. Lippens, J.H. De Boer, J. Catal. 4 (1965) 319.

[32] J.H. De Boer, B.C. Lippens, B.G. Lisen, B.C.P. Broekhoff, A. Van Den Heuvel, T.J. Osinga, J. Colloid Interface Sci. 21 (1966) 405.

[33] J. Lynch, F. Raatz, P. Dufresne, Zeolites 7 (1987) 333.

[34] S. Parinyakit and P. Worathanakul, *Static and Dynamic Simulation of Single and Binary Component Adsorption of CO2 and CH4 on Fixed Bed Using Molecular Sieve of Zeolite 4A*, Processes (2021), 9, 1250.